Structural Engineering and Mechanics, *Vol. 48, No. 4 (2013) 479-500*
DOI: http://dx.doi.org/10.12989/sem.2013.48.4.479

Lateral deformation capacity and stability of layer-bonded scrap tire rubber pad isolators under combined compressive and shear loading

Huma Kanta Mishra*[1] and Akira Igarashi[2a]

[1]Department of Urban Management, Kyoto University, Japan
[2]Department of Civil and Earth Resources Engineering, Kyoto University, Japan

(Received October 19, 2012, Revised October 10, 2013, Accepted October 26, 2013)

Abstract. This paper presents the experimental as well as analytical study conducted on layer-bonded scrap tire rubber pad (STRP) isolators to develop low-cost seismic isolators applicable to structures in developing countries. The STRP specimen samples were produced by stacking the STRP layers one on top of another with the application of adhesive. In unbonded application, the STRP bearings were placed between the substructure and superstructure without fastening between the contact surfaces which allows roll-off of the contact supports. The vertical compression and horizontal shear tests were conducted with varying axial loads. These results were used to compute the different mechanical properties of the STRP isolators including vertical stiffness, horizontal effective stiffness, average horizontal stiffness and effective damping ratios. The load-displacement relationships of STRP isolators obtained by experimental and finite element analysis results were found to be in close agreement. The tested STRP samples show energy dissipation capacity considerably greater than the natural rubber bearings. The layer-bonded STRP isolators serve positive incremental force resisting capacity up to the shear strain level of 150%.

Keywords: layer bonded STRP; compression test; cyclic shear test; FE analysis, low-cost base isolation

1. Introduction

Base isolation is the technique to reduce the seismic demand on structures instead of increasing the seismic resistant capacity of the structures. The reduction of seismic demand on structures can be achieved by providing a certain degree of flexibility in the structural system by installing isolation devices having low horizontal stiffness. Rubber bearings of different types, including lead rubber bearings, high damping rubber bearings and steel laminated rubber bearings are being used to serve this purpose. Nowadays, this technology has become an attractive alternative to the conventional seismic resistant design methods.

The problem with adopting isolation systems to structure in developing countries is that conventional isolators are large, expensive and heavy. To extend this earthquake resistant strategy to housing and commercial buildings, the weight and cost of the isolators must be reduced (Kelly

*Corresponding author, Ph.D., E-mail: humakanta@ymail.com
[a]Associate Professor, E-mail: igarashi.akira.7m@kyoto-u.ac.jp

http://www.techno-press.org/?journal=sem&subpage=8 ISSN: 1225-4568 (Print), 1598-6217 (Online)

2002). Experience of the past earthquakes in developing countries suggests that the seismic performance of the structure could be significantly improved by the introduction of a simple seismic isolation system either at the construction or during the retrofitting stage. This would result in fewer building failure and decreased loss of lives during the past earthquake events (Toopchi-Nezhad *et al*. 2008).

Although the base isolation has proven its effectiveness, the technology is still perceived as expensive and difficult to implement. Thus in the recent years, a new approach emerges in the academic world and this approach consists in developing a low-cost base isolation system in order to extend the use of this method in developing countries. A few studies have been conducted using either steel laminated rubber bearings (Kelly and Konstantinidis 2007) or fiber-reinforced elastomeric isolators (Kelly 2002, Toopchi-Nezhad *et al*. 2008, Mordini and Strauss 2008, Ashkezari *et al*. 2008) as low-cost base isolation systems for highly seismic regions of the world. These types of seismic isolators are still economically unacceptable considering the purchasing capacity of poor families in the developing countries. This research is intended to develop a low-cost seismic isolator having properties similar to commercially available seismic isolators in the context of the behavior except for axial load carrying and lateral deformation capacities.

The research on scrap tire pad has been initiated by Turer *et al*. (2008), in which, the researchers produced the specimen samples using car tires and tested in vertical compression and in cyclic shear. The experimental test was conducted by stacking the individual layer of STRP one on top of another without using chemical adhesive. Due to this reason, Turer *et al*. noticed the slippage problem which ultimately decreases the shear deformation capacity of the specimen. The authors suggested that the slippage problem could be overcome by inserting nails or making the surface rough. The car tire usually contents synthetic fiber as reinforcing cords which results in low vertical load capacity. This result appears to show that the examined STRP isolators were insufficient for the practical use of scrap tire rubber pad in building isolation.

In this study, the layer-bonded STRP specimen samples were produced by stacking STRP layers produced from the tread part of the scrap tires for bus/trucks one on top of another with the application of adhesive. The detailed description on the specimen sample preparation procedure is discussed in the following chapter. In the case of unbonded application, the stacked STRP shows roll-off behavior when subjected to lateral shear deformation with its upper and lower faces loose contact on the supports. This type of deformation decreases the effective horizontal stiffness of the isolator with the increase in lateral displacement. This phenomenon will include period elongation of the isolated system provided that the stability is maintained (Toopchi-Nezhad *et al*. 2011).

In this paper, the results of shear loading tests and finite element analysis (FE analysis) conducted on layer-bonded STRP isolators are presented. The experimental test results are used to determine the mechanical properties of the STRP isolator, including stiffness and damping ratios, as well as the stability limit state corresponding to the critical shear strain. These results are further compared with relevant and recent version of codes provisions (UBC 1997, Eurocode 8 2004, ASCE-7 2005) to check the viability of using layer-bonded STRP as seismic isolators. The FE analysis to simulate the shear loading test is conducted to verify the special features and character of the horizontal force-displacement relationships found in the shear loading test.

2. Layer- bonded STRP specimen samples

The STRP specimen samples are prepared in accordance with the procedure described in the

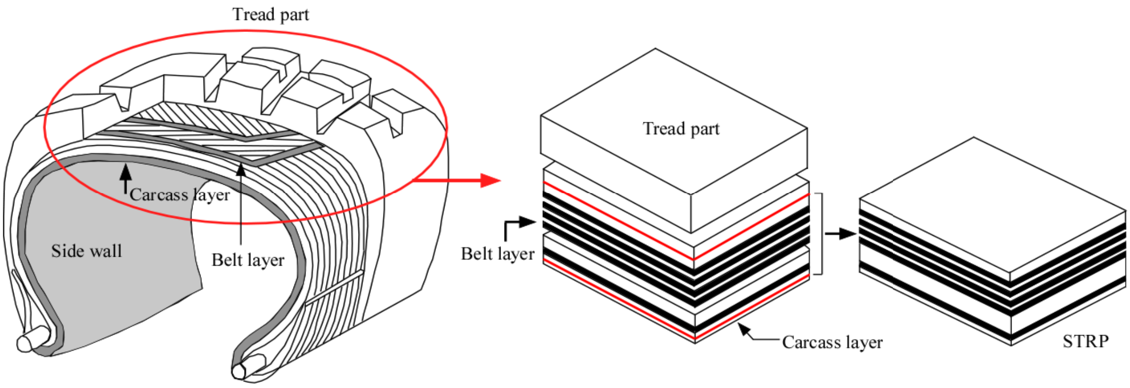

Fig. 1 STRP preparations using the tread part of the tire

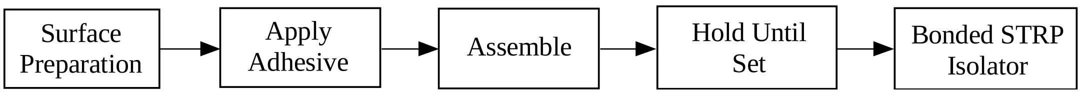

Fig. 2 Basic steps involved in the adhesive bonding of STRP layers

previous paper (Mishra *et al*. 2012). Only the rubber from the tread part of the tire is used as shown in Fig. 1. The tire product used for the preparation of STRP specimen samples is Bridgestone Tire, 385/65R22, 5.

2.1 Bonding of STRP layers using adhesive

The bonding between rubbers to rubber is generally achieved by using either epoxy or urethane. For the bonding of vulcanized rubber surfaces, epoxy is generally used as adhesive, in addition to essential application of priming, for which the type of primer depends on the rubber material and type of epoxy to be used. In the particular case of study, Chemlok 7701 and Fusor 320/322 (Lord Corp.) are used as the primer and the epoxy adhesive, respectively.

The raw STRP samples taken from a tire are sanded using a belt sanding machine as shown in Fig. 3, so that smooth plain surfaces are obtained on the STRP samples. The sanded STRP surfaces must be cleaned to achieve proper good quality adhesion between the surfaces. Foreign materials such as dirt, oil, moisture, rust, loose particles and any contaminants, if they exist, have to be removed from the surface; otherwise, the adhesive will bond to these weak boundary layers rather than to the substrate. These treatments generally involve physical process, typically with a hard brush, chemical process to apply appropriate agent, or combination of both. The choice of surface treatment process, recommended by the adhesive supplier, depends on the adhesive to be used. The chemical treatment of the surfaces by applying the Chemlok 7701 primer with a brush allows the surface to be more easily wet, which improves compatibility with adhesive and environmental resistance, thus making the rubber surfaces more receptive to bonding. After the solvent flashes off in approximately five minutes, the treatment is assumed to be complete. The bonding between STRP samples is conducted immediately after the solvent has flashed off to achieve the best adhesion quality in creating layer-bonded STRP samples. The basic steps followed in the preparation of the layer-bonded STRP sample is shown in Fig. 2.

The Fusor 320/322 contains resin and hardener compounds. The adhesive is prepared by mixing equal amounts of Fusor 320 and 322 by volume, as recommended by the manufacturer for general purpose (temperature range between -40℃ to 204℃) application. The prepared adhesive paste is applied on both sides of STRP surfaces using a spatula. The thickness of adhesive shall be around 0.5 mm to achieve proper bonding. The STRP samples are assembled into a layer-bonded STRP so that no air is entrapped in the bonding interfaces, and pressure (about 0.2 MPa) is applied to ensure good wetting of the adhesive on both surfaces. The layer-bonded STRP samples are placed undisturbed for 24 hours to achieve fully cured. Figs. 4 to 6 show the surface preparation, adhesive application and cured samples, respectively. The dimensions of the STRP samples are shown in Table 1. The overall thickness of STRP-4, produced by bonding four STRP samples, is increased by 2 mm due to the application of adhesive.

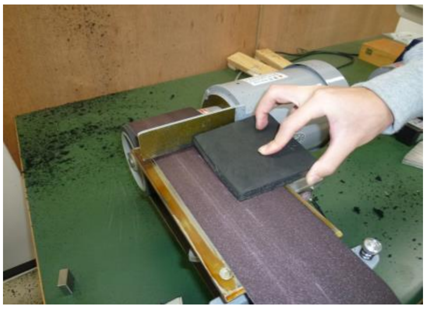

Fig. 3 Sanding of STRP layer is in progress

Fig. 4 Surface treatment by primer

Fig. 5 Single layer with adhesive on surface

Fig. 6 Fully cured layers bonded samples

Table 1 Geometrical properties of the layer-bonded STRP

Width of the STRP = 100 mm
Thickness of a single layer STRP = 12 mm
Thickness of steel reinforcing cords = 0.4 mm
Total thickness of STRP-4 = 48 mm, t_r = 40 mm
Thickness increased by adhesive = 2 mm

Table 2 Capacity of testing equipment

Actuator	Max. Displacement	Max. Load	Direction	Remarks
No.1	±100 mm	±100 kN	Horizontal	F_X
No.2	±100 mm	±100 kN	Horizontal	F_Y
No.3	±100 mm	±500 kN	Vertical	F_Z

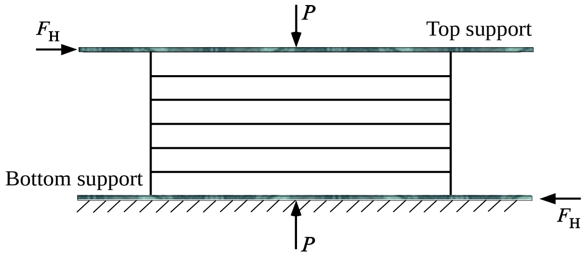

Fig. 7 Loading setup for STRP isolator

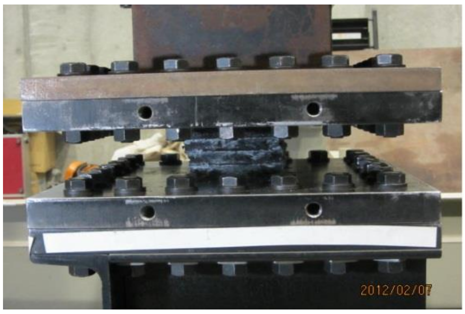

Fig. 8 STRP-4 and overall view of test set up (photograph)

3. Shear loading test

A shown in Fig. 7, a series of shear loading test of the layer-bonded STRP-4 specimens are conducted by applying horizontal force F_H under a vertical compression force P. Fig. 9 shows the schematics of the test setup using a three-dimensional loading equipment; two horizontal and one vertical loading, by means of servo-hydraulic actuators. The STRP-4 specimens are placed between the upper reaction frame and lower steel loading block as shown in Fig. 8. The vertical load is applied to the specimen by the vertical hydraulic actuator, with a maximum loading capacity of ±500 kN and maximum displacement capacity of ±100 mm, using a constant load control. The horizontal load is applied by imposing specified displacements by the horizontal hydraulic actuators with a load capacity of ±100 kN and a maximum displacement capacity of ±100 mm. The capacity of the testing equipment in all the three directions is presented in Table 2.

3.1 Preliminary axial compression test

In order to investigate the fundamental property of the layer-bonded STRP, two preliminary axial compression tests of the STRP-4 specimens are conducted. Results of the tests, ‘‘Test 1’’ and ‘‘Test 2’’ are described in this section.

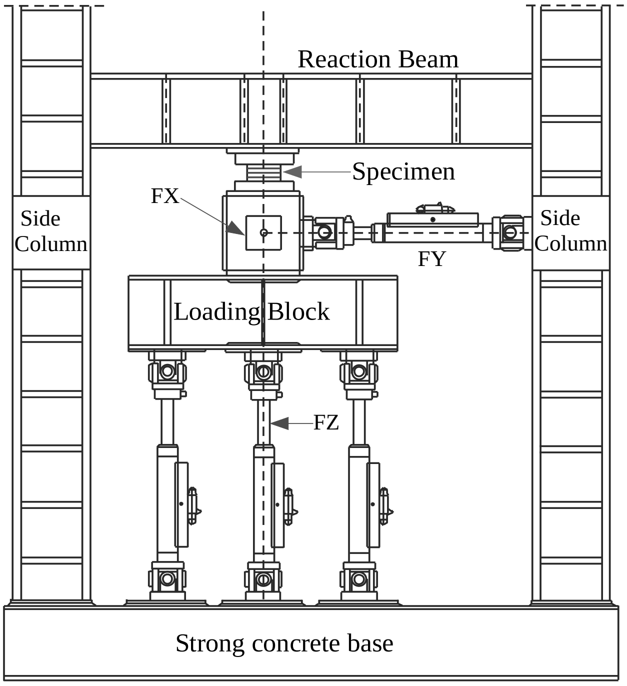

Fig. 9 Schematics of test setup and instrumentation

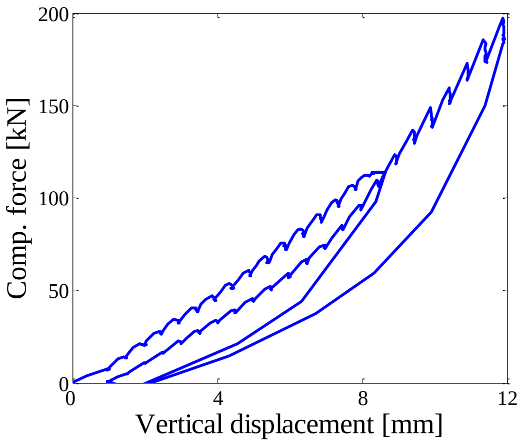

Fig. 10 Vertical load-deflection relationships of STRP-4 specimen in Test 1

3.1.1 Test 1

In Test 1, the initial condition is such that the sample was just made contact with the top and bottom support surfaces with zero vertical compression load. The vertical load was applied and increased until 120 kN, and then unloading was performed, and again the vertical load was increased up to 200 kN. This is equivalent to 20 MPa axial pressure on the STRP-4 specimen. The STRP-4 specimen did not show any sign of failure in Test 1. The force-displacement relationship obtained from Test 1 is shown in Fig. 10.

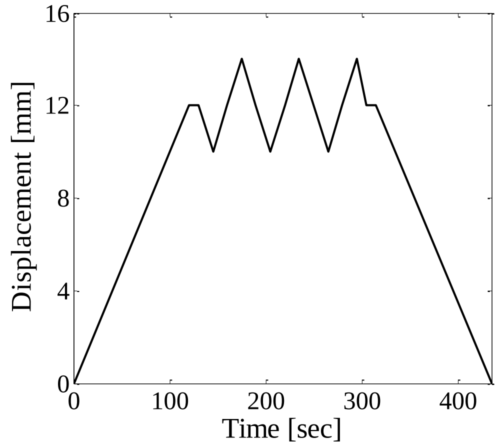

Fig. 11 Input signals

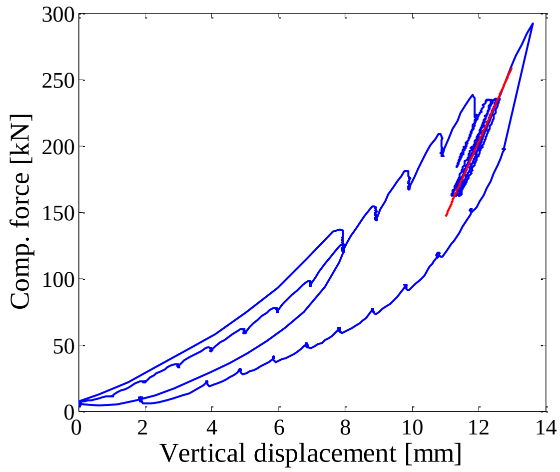

Fig. 12 Load-deflection relationship

3.1.2 Test 2

In Test 2, an STRP-4 specimen was tested in vertical compression, including a cyclic loading pattern at its maximum amplitudes. At the initial stage, the specimen was loaded up to an equivalent pressure of 13.7 MPa and unloaded. Then the compressive load was increased to 200 kN which is equivalent to 20 MPa axial pressures on the SRTP-4 specimen. Starting from this loading condition, three fully reversed cycles with ±4 MPa amplitude were performed. The loading history and force-displacement relationship in Test 2 is presented in Figs. 11 and 12.

The vertical stiffness value determined by the least square fitting technique to the load-displacement relationship obtained by Test 2 is calculated as $(K_V)_1$=56.417 MN/m. From this result, the effective compression modulus of the STRP-4 specimen as a monolithic rubber material model is E_1= 270.8 MPa. The vertical stiffness of the layer-bonded STRP-4 specimen is sufficient to withstand structural load of low-rise residential buildings and to prevent the rocking motion of the structure. An effective compression modulus of E_1= 270.8 MPa at an axial pressure of 5 MPa implies a vertical vibrational frequency of 18.4 Hz, which is sufficient for any seismic isolation system (Kelly 1997).

3.2 Cyclic shear test

3.2.1 Test S1

In Test S1, a STRP-4 specimen is tested in cyclic shear with three fully reversed cycles at three maximum shear displacement amplitudes of 20 mm, 40 mm and 60 mm, at constant vertical pressure of 10 MPa. The loading history in the horizontal shear test is shown in Fig. 13 and the force-displacement relationship obtained by Test S1 is presented in Fig. 14.

3.2.2 Test S2

In Test S2, an STRP-4 specimen is tested in cyclic shear with three fully reversed cycles at four maximum shear displacement amplitudes of 15 mm, 30 mm, 45 mm and 60 mm, at a constant vertical pressure of 5 MPa. The loading history in Test S2 is presented in Fig. 15. Fig. 16 shows the force-displacement relationship obtained by Test S2. The deformed states of the specimen at different shear strain levels are shown in Fig. 17. Although noticeable slip can be seen in Fig. 16 at the displacement amplitudes of 45 mm, this phenomenon again disappears for a higher level of displacement amplitudes.

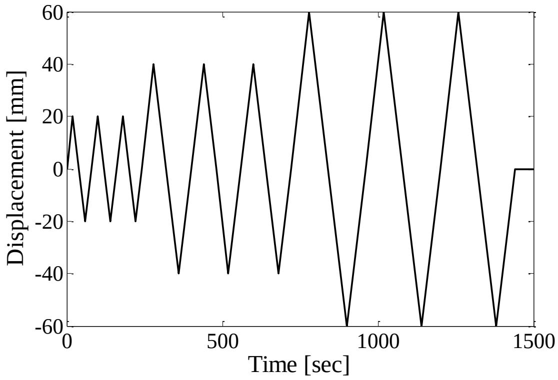

Fig. 13 Input signals for horizontal cyclic shear Test S1

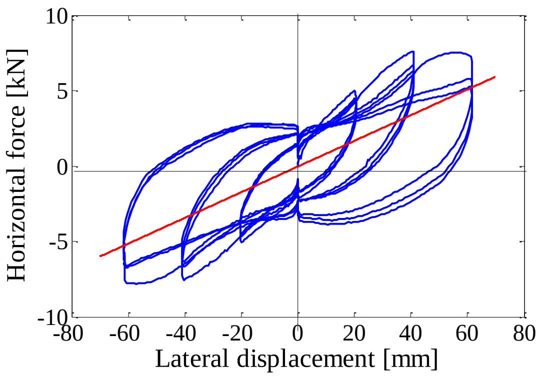

Fig. 14 Load displacement relationship in cyclic shear

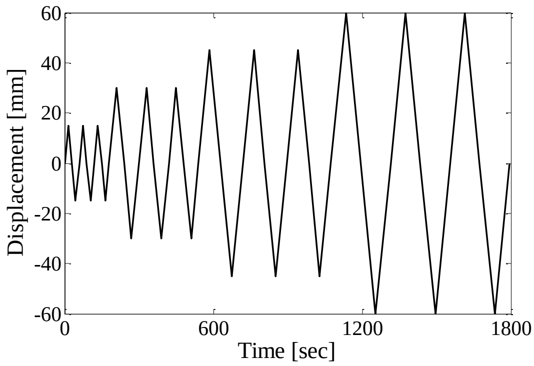

Fig. 15 Input signals for horizontal cyclic shear Test S2

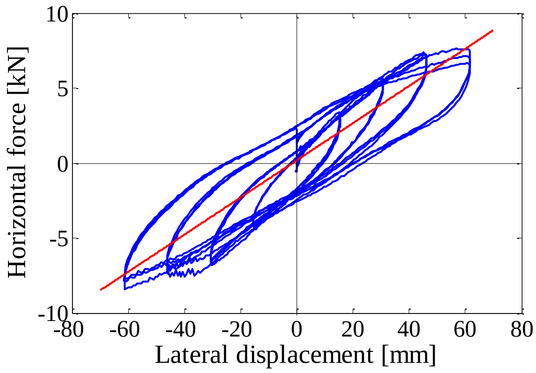

Fig. 16 Load-displacement relationship in Test S2

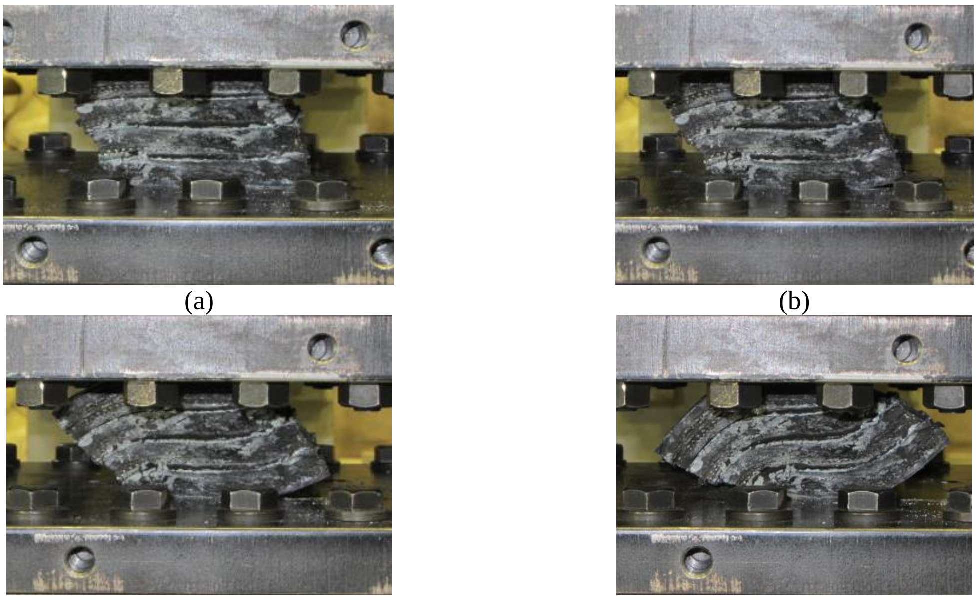

(a) (b)

(c) (d)

Fig. 17 Deformed state of layer-bonded STRP-4 specimen under constant 5 MPa vertical pressure subjected to (a) 37.5%, (b) 75%, (c) 112.5% and (d) 150% shear strain

Fig. 18 Deformed state of layer-unbonded STRP-6 specimen under constant vertical pressure of 5 MPa at 103% shear strain

The vertical stiffness of layer-unbonded STRP-6 specimen at 103% shear strain with vertical axial pressure of 5 MPa is about 20.7 MN/m which corresponds to effective compression modulus of 149.03 MPa. The corresponding vertical vibrational frequency is 11.2 Hz and is considered satisfactory value for seismic isolation purpose (Kelly 1997). Even though, the layer-unbonded STRP specimen produces sufficient vertical stiffness and provides shear strain of 103%, it is almost physically unstable due to the separation of STRP layers which is shown in Fig. 18. On the other hand, layer-bonded STRP specimen provides considerably higher level of vertical stiffness (56.41 MN/m) than the layer-unbonded STRP specimen. During the shear loading, none of the layer-bonded STRP-4 specimens show layer separation. The shear deformation capacity is largely increased due to the application of adhesive. The layer-bonded STRP-4 specimen is stable physically and characteristically to provide shear strain level of 150%. These results indicate the effectiveness of bonding of the STRP layers.

4. Horizontal stiffness of STRP-4 specimen

The STRP-4 specimen’s effective horizontal stiffness corresponding to each load cycle of the test can be calculated based on the peak lateral load and peak lateral displacement as follows (UBC 1997)

$$K_{eff} = \frac{F^{+} - F^{-}}{\Delta^{+} - \Delta^{-}} \tag{1}$$

where F^{+}, F^{-}, Δ^{+} and Δ^{-} are the positive/negative peak values of horizontal loads and horizontal displacements, respectively, at the extremes of the cyclic displacement range. For the last cycle of the tests, the effective horizontal stiffness of the layer-bonded STRP-4 specimen with 10 MPa and 5 MPa axial pressures at 150% shear strain is 127.4 kN/m and 132.3 kN/m, respectively. The average horizontal stiffness of the STRP isolators was evaluated using the least square fitting technique. The maximum lateral displacements as well as average horizontal stiffness values of STRP isolators are shown in Table 3. From Table 3, it can be seen that the average horizontal stiffness decreases with increase in axial pressure for equal level of horizontal displacement.

Table 3 Average horizontal stiffness of layers bonded STRP isolators

Test No.	Sample	Dimensions (mm)	Axial stress (MPa)	Hor. Displacement (mm)	Hor. stiffness (kN/m)
1	STRP-4	100x100x48	10.0	60	85.3
2	STRP-4	100x100x48	5.0	60	124.0

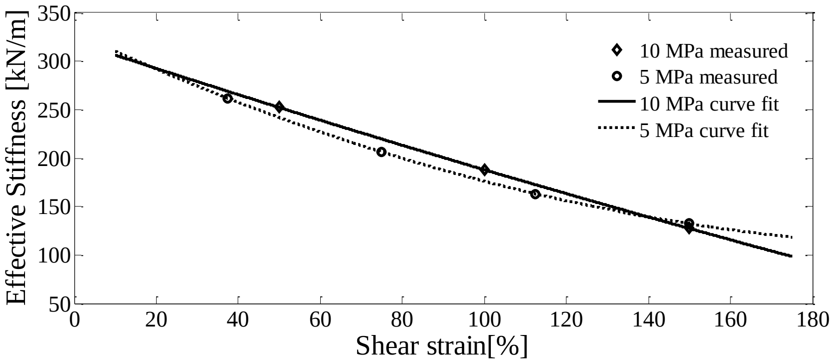

Fig. 19 Variation of effective stiffness with shear strain of STRP-4 at different axial pressures

The results of experimental test are used to determine the effective horizontal stiffness at the maximum shear displacement amplitudes. Due to the rollover deformation, the effective horizontal stiffness decreases with increase in lateral displacement which further elongates the period of the isolation system. Fig. 19 shows that the variation of the stiffness can be approximated as a linear function for a larger axial pressure (10 MPa) whereas the variation is nonlinear for lower axial pressure (5 MPa).

5. Effective damping of STRP-4 specimen

The effective damping (β_{eff}) of an isolator shall be calculated for each cycle of loading by the formula (UBC 1997)

$$\beta_{eff} = \frac{2}{\pi}\left[\frac{E_{Loop}}{K_{eff}\left(\left|\Delta^{+}\right| + \left|\Delta^{-}\right|\right)^{2}}\right] \tag{2}$$

where E_{Loop} is the energy dissipated per cycle of the loading, Keff is the effective horizontal stiffness.

Using the quantities for 60 mm lateral displacement as the peak amplitude, the average effective damping ratio for axial pressure of 10 MPa and 5 MPa are calculated as 0.18 and 0.15, respectively. When axial pressure drops to 3.3MPa, the average effective damping ratio is approximately 0.10. These effective damping ratios are slightly higher than the effective damping ratio obtained from layer-unbonded STRP specimen tests (0.12 at 80% shear strain with the axial pressure of 5 MPa). The damping ratio also depends on axial pressure on the STRP specimens.

The effective damping ratio is evidently higher than the natural rubber bearings for which the equivalent damping is usually 2 to 3 % (Naeim and Kelly 1999). The relationship between shear strain and effective damping is shown in Fig. 20 for the entire range of lateral displacement.

The test result shows that the adhesive bonding is sufficiently strong to withstand the shear strain of 150%. The tests conducted with larger axial pressure (10 MPa) and with low axial pressure (3.3 MPa) show that the layer-bonded STRP specimens are especially suitable for lightly loaded building structures. Fig. 18 shows that the horizontal effective stiffness of the layer-bonded STRP specimen significantly reduces as the horizontal displacement increases. This phenomenon can be attributed to the unbonded contact condition of the layer-bonded STRP specimen with the top and bottom support interfaces. The decrease in horizontal stiffness consequently increases the isolation period, provided that the stability of the isolation bearing as well as whole building structure is maintained. Fig. 20 reveals that the effective damping value also depends on the axial pressure as well as horizontal displacement.

Fig. 21 clearly shows that the force-displacement relationship in the 5 MPa axial pressure case has positive incremental force resisting capacity up to 60 mm displacement which is equivalent to 150% shear strain. From this figure, it can be concluded that 10 MPa axial stresses can be applied to achieve 100% shear strain, beyond which the STRP specimen is considered to be unstable (UBC 1997, ASCE-7 2005).

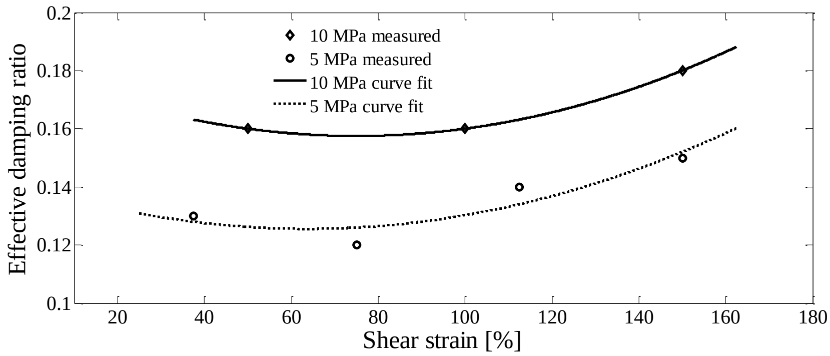

Fig. 20 Variation of effective damping with shear strain

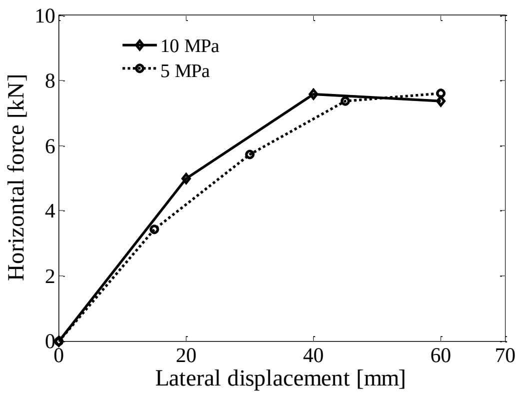

Fig. 21 Comparison of force-displacement relationship for various axial pressures

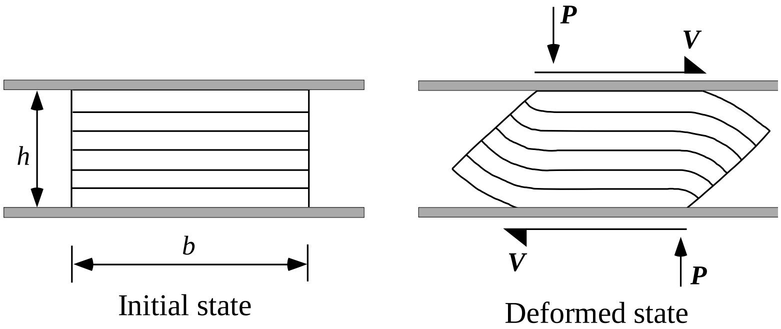

Fig. 22 Free body diagram of laterally deformed layer-bonded STRP isolator

6. Finite element analysis

The FE analysis of a strip layer-bonded STRP-4 specimen is carried out to assess the force-displacement behavior and to evaluate the stress state within the specimen when it is used as seismic isolator. The sketch of the deformation pattern of the layer-bonded STRP as a seismic isolator with unbonded application between the superstructure and substructure is shown in Fig. 22. In this case, the moment created by the offset of the resultant compressive force *P* balances the moment created by the shear force *V*, no or negligible tensile stresses are produced within the STRP isolator.

6.1 Modeling of layer-bonded STRP

The layer-bonded STRP to be used as seismic isolator is composed of a rubber body with embedded steel reinforcing cords. The layer-bonded STRP's geometrical properties are given in Table 1. Finite element analysis of the strip layer-bonded STRP was conducted using commercially available general purpose finite element software (MSC software 2010). The rubber was modeled with four-node, isoparametric quadrilateral elements coded for plane strain incompressible applications. This element is preferred over higher-order elements when used in simulating large deformation and contact analysis (MSC volume A 2010). The reinforcing steel cords were modeled by using the isoparametric plane strain two-node line elements, which is referred to as rebar elements, to be used in conjunction with four-node plain strain continuum elements (host elements). These rebar elements have to be embedded into their corresponding solid elements representing the matrix materials. Since the matrix element and the rebar element share the same nodal points, no additional degrees of freedom are introduced. The degree of freedom of the nodes to be inserted is tied to the corresponding degree of freedom of the host elements. When defining the material properties of the rebar layer, the reference plane or the edge of the rebar layer should be defined. In this model, the reference axis of the rebar direction, the cross-section area of a single rebar, density/spacing of the rebar, angle of orientation with respect to the reference axis are defined.

For the top and bottom layers, the edge length of the quadrilateral elements is selected to be approximately 0.4 mm, while the element edge length for intermediate layers is approximately 0.5 mm. The number of quadrilateral and rebar elements in a single layer of STRP placed near the uppermost and lowermost support surfaces are 8750 and 1250, respectively. The numbers of

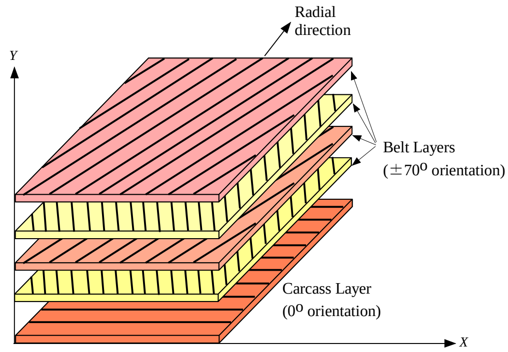

Fig. 23 Layout of steel reinforcing cords in a single layer of STRP

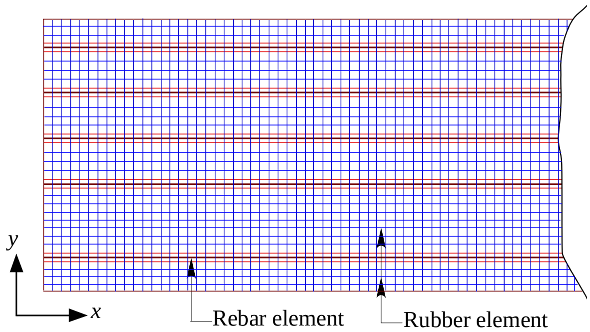

Fig. 24 Finite Element mesh in a single layer of STRP

quadrilateral and rebar elements in the middle layers are reduced to 5800 and 1000, respectively. There are total of 33600 elements in a layer-bonded STRP-4 model. The area of a single steel reinforcing cord in carcass layers is 0.44 mm^2, while that in the belt layer is 0.63 mm^2. The spacing of the steel reinforcing cords is approximately 0.4/mm. The orientation of the rebar direction in the belt layer is assigned as ± 70° with respect to the direction of the cords in the carcass layer (Wong 2001), as shown in Fig. 23. The typical finite element meshing for a single layer STRP is shown in Fig. 24. The rubber is represented by a hyperelastic material model while the steel reinforcing cords are treated using a linear elastic isotropic material with Young's modulus E= 200 GPa and Poisson's ratio v= 0.3.

In this model, the vertical and horizontal loads are applied on the top support; the top support is allowed to move in the vertical and horizontal directions without rotation while the bottom support is considered as a fixed support. The contact between the supports and the layer-bonded STRP is modeled by the Coulomb friction law with a coefficient of friction 0.8. The coefficient of friction was selected such that no slips occur between the contact support and the rubber interfaces. The layer-bonded STRP is allowed for roll off the contact supports implying that the nodal points were allowed to detach from the contact supports when the compression contact stresses approach to zero.

Generally, the rubber is regarded as isotropic hyperelastic material that can be represented by constitutive law expressed in terms of strain energy density function. Among the various constitutive models, the Mooney-Rivlin model is commonly used to characterize the rubber material undergoing large strain (Ali *et al*. 2010). This model is the simplest hyperelastic model

Table 4 Mooney-Rivlin material constants

Material constants (MPa)		
C_{10}	=	0.40
C_{01}	=	1.22315
C_{11}	=	0.18759

for elastomeric materials when material test data is insufficient. The Mooney-Rivlin material law is well suited for most practical applications involving cord-reinforced rubber material (Helnwein *et al*. 1993). The strain energy polynomial is expressed as

$$W = \sum_{i,j=0}^{N} C_{ij}(I_1 - 3)^i (I_2 - 3)^j + \sum_{i=1}^{N} \frac{1}{D_i}(J_{el} - 1)^{2i} \tag{3}$$

where C_{ij} and D_i are material parameters that are found from test data, J_{el} is the elastic volume ratio, I_1 and I_2 are the invariants of the green deformation tensor given in terms of the principal stretch ratios λ_1, λ_2 and λ_3 by

$$I_1 = \lambda_1^2 + \lambda_2^2 + \lambda_3^2 \tag{4}$$

$$I_2 = \lambda_1^2\lambda_2^2 + \lambda_2^2\lambda_3^2 + \lambda_3^2\lambda_1^2 \tag{5}$$

where λ_1, λ_2 and λ_3 are the stretch ratios in principal directions. In Eq. (3), the first summation is the contribution due to deviatoric effects and the second summation is the contribution due to volumetric effects. The volumetric strain in the finite element is nearly zero in a nearly incompressible material. The earliest phenomenological theory of nonlinear elasticity was proposed by Mooney-Rivlin as

$$W = C_{10}(I_1 - 3) + C_{01}(I_2 - 3) \tag{6}$$

Although, it shows a good agreement with tensile test data up to 100% strains, it has been found inadequate in describing the compression mode of deformation. Moreover, the Mooney-Rivlin material model expressed by Eq. (6) fails to account for the hardening of the material at large strains (MSC software 2000). The retention of the third term in the Mooney-Rivlin strain energy density function lead to better agreement with test data and stress-strain behavior can be described with excellent accuracy up to breaking stage of the specimen (Tschoegl 1971).
Three terms Mooney-Rivlin strain energy density function can be expressed as

$$W = C_{10}(I_1 - 3) + C_{01}(I_2 - 3) + C_{11}(I_1 - 3)(I_2 - 3) \tag{7}$$

where C_{10}, C_{01} and C_{11} are the material constants known as Mooney-Rivlin material constants. The hyperelastic material constants used in FE analysis were derived by conducting uniaxial tension tests (Mishra *et al*. 2011). In this work, the strain energy density function expressed by Eq. (7) was utilized with material constants given in Table 4.

6.2 Loads

In the analysis, loads are applied to the model in an incremental manner in order to capture the nonlinear behavior of the cord-rubber composite. At the initial stage of the analysis, the target vertical load corresponding to compressive pressure of 5 MPa or 10 MPa is applied in different incremental steps. Then the horizontal load is applied with the constant compressive load until a target lateral displacement is achieved. The target lateral displacement is selected such that 150% shear deformation in the layer-bonded STRP-4 is achieved.

6.3 Finite element analysis of layer-bonded STRP

The FE analysis of layer-bonded STRP is carried out for the case of application unbonded with the support surfaces. This type of seismic isolation system allows for rollover deformation to take place in the layer-bonded STRP used as the isolator. When the rollover deformation occurs one end of the isolator separates from the contact support while the other end is highly stressed as shown in Figs. 25 (a) and 26 (a). The corresponding shear strain distribution within the layer-bonded STRP is shown in Figs. 25 (b) and 26 (b), respectively.

The analysis was two-dimensional under the plane strain assumption. The low value of shear modulus of rubber causes the deformation pattern relatively severe as compared with other materials like steel and concrete. Its large deformability together with its near-incompressibility makes rubber a major challenge for finite element analysis. The large deformation that the rubber components experience can only be modeled with a finite strain formulation (Kelly and Konstantinidis 2007).

In large deformation analysis of elastomeric materials, two equivalent methods may be used: the total Lagrangian method and updated Lagrangian method. In the total Lagrangian approach, the equilibrium is expressed with the original undeformed state as the reference; in the updated Lagrangian approach, the current configuration acts as the reference state (MSC volume A 2010). Generally, elastomeric materials undergo very large deformation under shear loading. In this case, it is necessary to update the orientation of the local coordinate system based on the deformed configuration of the element during the analysis. Due to this reason, updated Lagrangian approach is used in the FE analysis of layer-bonded STRP.

In 2D finite element model, for each rubber element, local axes can be denoted by axis 1 and axis 2 which are parallel and perpendicular to the orientation of the carcass layer, respectively.

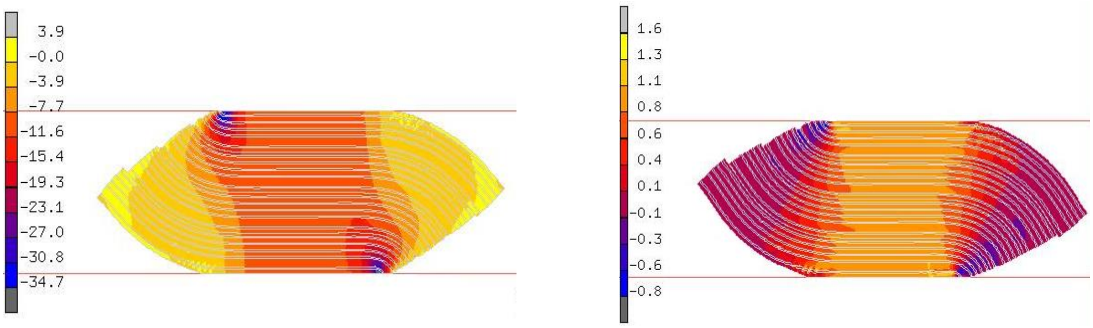

(a) Contour of normal stress S_{22} (MPa) (b) Shear strain distribution

Fig. 25 Normal stress and shear strain distribution in the rubber layers of the STRP-4 model under axial pressure of 5 MPa

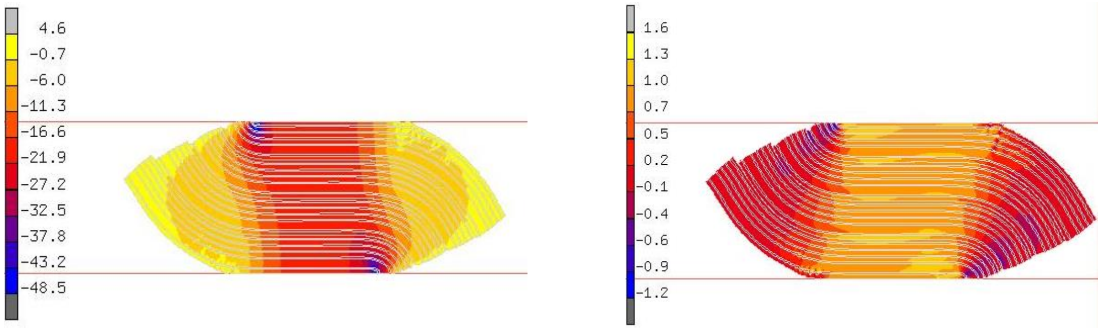

(a) Contour of normal stress S_{22} (MPa) (b) Shear strain distribution

Fig. 26 Normal stress and shear strain distribution in the rubber layers of the STRP-4 model under axial pressure of 10 MPa

The normal stress S_{11} acts parallel to the orientation of steel reinforcing cords in carcass layer while normal stress S_{22} acts perpendicular to the reinforcing cords in carcass layer. Due to the unbonded application with support interfaces, the STRP is allowed to roll off the contact supports which results in shifting the line of action of vertical load resultant, at each contact surface as shown in Fig. 22. As a result, no balancing moment develops at the top and bottom surfaces of layer-bonded STRP. The lower level of tension stress S_{22} as shown in Figs. 25(a) and 26(a) in the layer-bonded STRP prevents the peeling of STRP layers at extreme shear deformation level. The compression zone is responsible to carry the vertical compressive load. As shown in Fig. 25 and 26, the bonding of STRP layers using adhesive is strong enough to transmit the stresses and to prevent the tangential motion between the STRP layers.

For the efficient operation of elastomeric isolator, the shear strain in the rubber material must be extremely large (Toopchi-Nezhad *et al*. 2011).The shear strain in layer-bonded STRP is approximated as 1.5 and the maximum shear strain is in reasonable agreement with the maximum values given in Figs. 25(b) and 26(b).

The finite element analysis using the conventional lower-order isoparametric finite elements not tailored for incompressibility analysis produces extremely poor results (Kelly and Konstantinidis 2007), occasionally involving the volumetric mesh-locking (MSC software 2000). The mixed methods, in which both stress and strains are treated as known, are used in modern finite element analysis of incompressible and nearly incompressible materials (Zienkiewicz *et al*. 2005). The results of finite element analysis presented in this paper are based on the widely popular mixed method proposed by Herrmann (Herrmann 1965).

6.4 FE analysis results and discussion

The FE analysis was carried out on the strip layer-bonded STRP-4 model whereas the experimental tests were conducted on a square layer-bonded STRP-4 specimen. The lateral load-displacement relationship of the layer-bonded STRP is nonlinear as shown in Figs. 27 and 28. These figures contain lateral load-displacement relationships for the tests and the FE analysis of layer-bonded STRP-4 up to 150% shear strain. As shown in Figs. 27 and 28, reasonable agreement between the experimental tests and FE analysis results can be found. However, it should be noted that for a higher level of lateral displacement, the horizontal force obtained by the FE analysis is noticed to be higher than the experimental test results in both cases. Fig. 29 contains lateral load-displacement relationships obtained by FE analysis of layer-bonded STRP-4 up to 150% shear deformation for different axial pressures.

Figs. 25 (a) and 26 (a) show the distribution of normal stress (22-component) corresponding to 150% shear deformation in the layer-bonded STRP-4 for 5 MPa and 10 MPa axial pressures, respectively. As seen in Figs. 25 (a) and 26 (a), as a result of rollover deformation, high level stresses are induced at the corner region, while the stresses are relatively lower in the other region. Almost negligible tensile stresses are transferred to a laterally deformed STRP at the isolator's contact supports. As a result, no balancing moment develops at the top and bottom surfaces of a STRP isolator. The stability of the isolator entirely depends on the contact area between the isolator and the support surfaces at its maximum shear deformation level.

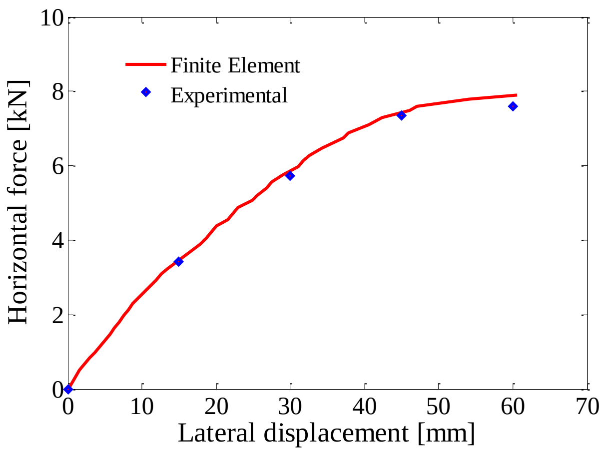

Fig. 27 Lateral load-displacement relationship of STRP-4 with 5 MPa axial pressure: comparison between experimental and FE analysis results

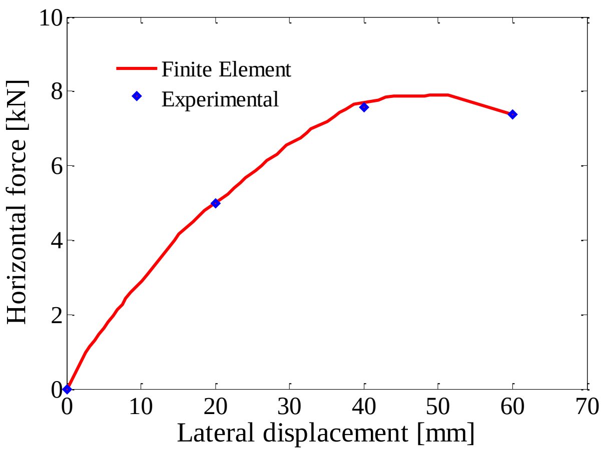

Fig. 28 Lateral load-displacement relationship of STRP-4 with 10 MPa axial pressure: comparison between experimental and FE analysis results

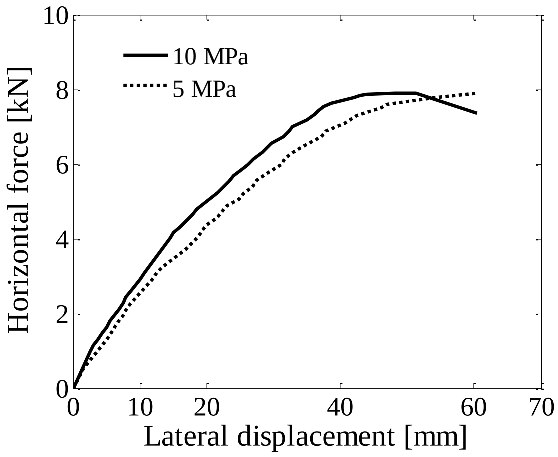

Fig. 29 Lateral load-displacement relationship of STRP-4 obtained by FE analysis for different axial pressures

For efficient operation of an elastomeric isolator, the shear strain in the rubber material must be extremely large. Figs. 25 (b) and 26 (b) illustrate the contour of shear strain within the isolators corresponding to 150% shear deformation in the layer-bonded STRP-4 for 5 MPa and 10 MPa axial pressures, respectively. As seen in Figs. 25 (b) and 26 (b), in the regions of the STRP-4 that are not in contact with the supports, the shear strain is found to decrease from its peak positive value. At extreme displacements, the shear strain acquires negative values in the STRP-4 at regions close to the ends of the rubber layer. The main purpose of steel reinforcement in a STRP is to restrain the lateral bulging of the rubber layers when the isolator is subjected to vertical loads. When a STRP isolator is loaded vertically, the rubber layers, which are confined by the steel reinforcement layers, undergo compression and the steel reinforcement layers in turn experience tension.

The contact interface between the outer layer of STRP and the contact supports is modeled as touching contact in both the cases. In this contact model, the shear force is transmitted through a Coulomb friction mechanism, while the normal force is transmitted across link. The shear force between the individual layers of layer-unbonded STRP is also transmitted through a Coulomb friction mechanism. The coefficient of friction is selected such that the layer separation is allowed and excessive slip is prevented. On the other hand, the individual layer of layer-bonded STRP is modeled as glue contact. In this contact model, the degrees of freedom of the contacting nodes are tied. This contact model prevents any detachment or slip between the individual layers of layer-bonded STRP by constraining the nodal points in the directions normal and tangential to the touching surfaces. The close agreement between the deformed state in shear loading tests and FE analysis verifies the present finite element model.

7. Discussion on applicability of layer-bonded STRP isolator

The isolation bearings are generally used at axial pressure levels ranging from 5 to 7 MPa (Kelly 1997). The compressive stress on isolators was between 3 and 8 MPa in the early years in

Japan (Pan *et al*. 2005). Due to the improved performance of the isolators, the compressive pressure is increased to 7-13 MPa for natural rubber bearings and 5-10 MPa for high damping rubber bearings. These isolators are generally adopted in multi-story building structures where the anticipated compressive load is much larger than the residential building. The average axial load on each of the columns of a three-story reinforced concrete building is estimated as 300 kN. The expected average axial pressure on layer-bonded STRP isolators is about 3-7 MPa in order to achieve 150% shear strain, as demonstrated by the test and analysis in the previous sections. The analytical study on stability of bonded STRP isolators (Mishra *et al*. 2012), reveals that these types of layer-bonded STRP can provide positive force resisting capacity up to 150% shear strain when loaded with axial pressure of 8.6 MPa. In this regards, the layer-bonded STRP can serve the purpose of base isolators for low-rise residential buildings. An interesting factor, however, is the level of damping shown by the STRP isolators. Figure 20 shows that the equivalent damping ratio that depends on the shear strain amplitude is always greater than 0.10 in any case. It is a favorable aspect of the use of layer-bonded STRP as seismic isolators to conform isolation design philosophy to reduce the seismic demand using the effect of energy dissipation mechanism of the spectrum system.

The production cost of a single layer of STRP is about 12 dollars. The total cost including adhesive chemical of a layer-bonded STRP-4 is about 68 dollars in Japan. Similar type of specimen can be produced in developing countries in the order of one fifth of the cost of Japan. The most important features of these bearings are the domestic production, they do not have steel end-plates and no extra cost is required for connection system. However their cost is in the hundreds of dollars as compared to the cost of commercially available seismic isolators in the thousands of dollars.

8. Conclusions

Experimental tests as well as FE analysis are conducted on layer-bonded STRP intended to be used as seismic isolators. The aim of the study is to investigate the behavior of layer-bonded STRP in static compression and in cyclic shear loading and to discuss the feasibility of the application to seismic isolators. The results of shear loading tests are used to determine the characteristic quantities of the layer-bonded STRP isolator. Two different levels of axial loads are applied during the shear loading tests and FE analysis to investigate the load-displacement behavior and to identify the stability of the layer-bonded STRP. During the shear deformation, none of the samples show layer separation. This result indicates that the bonding agent is sufficiently strong in transmitting the shear forces.

The properties of layer-bonded STRP are further compared with the relevant and recent codes provisions in order to identify the viability of the proposed base isolation system. The layer-bonded STRP provide positive incremental force resisting capacity up to shear strain level of 150% when loaded with 5 MPa axial loads. The ratio between vertical stiffness and horizontal stiffness is greater than 150 in any case, so that the layer-bonded STRP can be considered as feasible base isolation device (Eurocode 8 2004). It can be concluded that the layer-bonded STRP with axial pressure of 5 MPa can be used as the seismic isolator to achieve 150% shear strain while the shear deformation capacity sharply decreases to 100% when loaded with 10 MPa axial pressures. Another advantage of unbonded application of layer-bonded STRP with support surfaces is the roll over deformation, which decreases the effective stiffness of the isolator which further elongates the period of the isolation system provided that the stability is maintained. This type of seismic isolation system is intended to be used for low axial pressure application. Finally, it can be concluded that the low-cost base isolation system can be achieved by using STRP.

Acknowledgements

The authors would like to gratefully acknowledge Tokai Rubber Industries Ltd. Japan, for their valuable advice in the preparation of STRP specimen samples.

References

Ahmet, T. and Bayezid, Ö. (2008), “Seismic base isolation using low-cost Scrap Tire Pads (STP)”, *Materials and Structures*, **41**(5), 891-908.

Ali, A., Hosseini, M. and Sahari, B.B. (2010), “A review of constitutive models for rubber-like materials”, *American J. of Engineering and Applied Science*, **3**(1), 232-239.

ASCE-7 (2005), Minimum design loads for building and other structures, ASCE/SEI 7-05, New York, American Society of Civil Engineers.

Ashkezari, G.D., Aghakouchak, A.A. and Kokabi, M. (2008), “Design, manufacturing and evaluation of the performance of steel like fiber reinforced elastomeric seismic isolators”, *Journal of Material Processing Technology*, **197**(1-3), 140-150.

Eurocode 8 (2004), Design of Structures for Earthquake Resistance.

Helnwein, P., Liu, C.H., Meschke, G. and Mang, H.A. (1993), “A new 3-D finite element model for cord-reinforced rubber composites-Application to analysis of automobile tires”, *Finite Elements in Analysis and Design*, **14**(1), 1-16.

Herrmann, L.R. (1965), “Elasticity equations for incompressible and nearly incompressible materials by variational theorem”, *AIAA Journal*, **3**(10), 1896-1900.

Kelly, J.M. (1997), *Earthquake-resistant Design with Rubber*, 2nd Edition, Springer-Verlag, London.

Kelly, J.M. (2002), “'Seismic isolation system for developing countries”, *Earthquake Spectra*, **18** (3), 385-406.

Kelly, J.M. and Konstantinidis, D. (2007), “Low-cost seismic isolators for housing in highly-seismic developing countries”, *10th World Conference on Seismic Isolation, Energy Dissipation and Active Vibrations Control of Structures*, Istanbul, Turkey, May.

Mishra, H.K. and Igarashi, A. (2012), “Experimental and analytical study of scrap tire rubber pad for seismic isolation”, *World Academy of Science, Engineering and Technology*, Issue 62, (*Proc. International Conference on Earthquake and Structural Engineering*), Kuala Lumpur, February.

Mishra, H.K., Igarashi, A. and Matsushima, H. (2011), “Finite element analysis of scrap tire rubber pads as base isolation device”', *Proc. 24th KKCNN Symposium on Civil Engineering*, Hyogo, December.

Mishra, H.K., Igarashi, A. and Matsushima, H. (2012), “Finite element analysis and experimental verification of the scrap tire rubber pad isolator”, *Bulletin of Earthquake Engineering*, **11**(2), 687-707.

Mordini, A. and Strauss, A. (2008), “An innovative earthquake isolation system using fiber reinforced rubber bearings”, *Engineering Structures*, **30** (10), 2739-2751.

MSC Software (2008r1), MSC Marc 2010 and MSC Marc Mentat 2010, Santa Ana, California.

MSC. Marc (2010), Theory and user information, Vol. A Santa Ana, CA, MSC Software Corporation Inc.

MSC Software (2000), Nonlinear Finite Element Analysis of Elastomers, Whitepaper Santa Ana, California.

Naeim, F. and Kelly, J.M. (1999), *Design of Seismic Isolated Structures from Theory to Practice*, John Willey and Sons, Inc.

Pan, P., Zamfirescu, D., Nakashima, M., Nakayasu, N. and Kashiwa, H. (2005), “Base-isolation design practice in Japan: Introduction to the post Kobe approach", *Journal of Earthquake Engineering*, **9**(1), 147-171.

Toopchi-Nezhad, H., Tait, M.J. and Drysdale, R.G. (2008), "Testing and modeling of square carbon fiber-reinforced elastomeric seismic isolators", *Structural Control and Health Monitoring*, **15**(6), 876-900.

Toopchi-Nezhad, H., Tait, M.J. and Drysdale, R.G. (2011), "Bonded versus unbonded strip fiber reinforced elastomeric isolators: Finite element analysis", *Composite Structures*, **93**(2), 850-859.

Tschoegl, N.W. (1971), "Constitutive equations for elastomers", *Journal of Polymer Science Part-A: Polymer Chemistry*, **9**(7), 1959-1970.

Uniform Building Code (UBC) (1997), Volume 2, Structural Design Requirements, Earthquake Regulations for Seismic Isolated Structure, Whittier, CA.

Wong, J.Y. (2001), *Theory of Ground Vehicle*, 3rd Edition, John Wiley and Sons, Inc.

Zienkiewicz, O.C., Taylor, R.L. and Zhu, J.Z. (2005), *The Finite Element Method: Its Basis and Fundamentals*, 6th Edition, Butterworth-Heinemann, Oxford.